32nd Annual International Conference of the IEEE EMBS
Buenos Aires, Argentina, August 31 - September 4, 2010

Optimality in Neuromuscular Systems

Evangelos Theodorou and Francisco J. Valero-Cuevas

***Abstract*— We provide an overview of optimal control methods to nonlinear neuromuscular systems and discuss their limitations. Moreover we extend current optimal control methods to their application to neuromuscular models with realistically numerous musculotendons; as most prior work is limited to torque-driven systems. Recent work on computational motor control has explored the used of control theory and estimation as a conceptual tool to understand the underlying computational principles of neuromuscular systems. After all, successful biological systems regularly meet conditions for stability, robustness and performance for multiple classes of complex tasks. Among a variety of proposed control theory frameworks to explain this, stochastic optimal control has become a dominant framework to the point of being a standard computational technique to reproduce kinematic trajectories of reaching movements (see [12])**

In particular, we demonstrate the application of optimal control to a neuromuscular model of the index finger with all seven musculotendons producing a tapping task. Our simulations include 1) a muscle model that includes force- length and force-velocity characteristics; 2) an anatomically plausible biomechanical model of the index finger that includes a tendinous network for the extensor mechanism and 3) a contact model that is based on a nonlinear spring-damper attached at the end effector of the index finger. We demonstrate that it is feasible to apply optimal control to systems with realistically large state vectors and conclude that, while optimal control is an adequate formalism to create computational models of neuromusculoskeletal systems, there remain important challenges and limitations that need to be considered and overcome such as contact transitions, curse of dimensionality, and constraints on states and controls.

I. INTRODUCTION

The anatomical and physiological properties of muscle dynamics and musculo-skeletal structures naturally lead to nonlinear models for neuro-musculo-skeletal systems. Furthermore, the physiology and neural control of muscle tissue leads to stochasticity of neural commands and muscle activation (for a review please see [12]). Here we provide an overview of control methods applicable to such nonlinear stochastic models, and present extensions to these theories using an anatomically-realistic, tendon driven model of the index finger.

II. MODEL BASED STOCHASTIC OPTIMAL CONTROL METHODS

To capture this complexity, nonlinearities, and noise of these neuro-musculo-skeletal systems in mathematical terms, we consider the nonlinear stochastic dynamics of the form:

$$\mathbf{dx} = f(\mathbf{x},\mathbf{u})dt + F(\mathbf{x},\mathbf{u})\mathbf{d}\omega \tag{1}$$

where $\mathbf{x} \in \Re^{n\times 1}$ is the state, $\mathbf{u} \in \Re^{m\times 1}$ is the control and $\omega \in \Re^{p\times 1}$ Brownian motion noise with variance $\sigma^2 I_{p\times p}$. To capture the different sources of randomness in the nervous system we are assuming state and control dependent noise and therefore the term $F(\mathbf{x},\mathbf{u})$ is a function of state $\mathbf{x}$ and controls $\mathbf{u}$.

In stochastic optimal control theory, the goal is to find the control policy which minimizes a cost functions subject to the stochastic dynamics (1). The cost function is given by the equation that follows:

$$J^{\pi}(\mathbf{x},t) = E\left[h(\mathbf{x}(T)) + \int_{t_0}^{T} \ell\left(\tau,\mathbf{x}(\tau),\pi(\tau,\mathbf{x}(\tau))\right)d\tau\right]$$

The term $h(\mathbf{x}(T))$ is the terminal cost in the cost function while the $\ell(\tau,\mathbf{x}(\tau),\pi(\tau,\mathbf{x}(\tau)))$ is the instantaneous cost rate which is a function of the state $\mathbf{x}$ and control policy $\pi(\tau,\mathbf{x}(\tau))$. The cost $J^{\pi}(\mathbf{x},t)$ is defined as the expected cost accumulated over the time horizon $(t_0,...,T)$ starting from the initial state $\mathbf{x}_t$ to the final state $\mathbf{x}(T)$. The optimal cost or value function is defined as:

$$V(\mathbf{x},t) = \min_{\mathbf{u}} J^{\pi}(\mathbf{x},\mathbf{u},t)$$

The expectation above is taken over the noise ω. With respect to classical optimization methods, stochastic optimal control can be seen as a constrained optimization problem where the constrains corresponds to stochastic dynamics of the system. From the control theoretic point of view, optimal control is a principled way to find control policies that will not only stabilize a system around a desired behavior but will also achieve the desired task by minimizing some performance criterion.

Therefore, in stochastic optimal control theory the stochastic dynamics and the cost function to minimize are the essential components of the overall mathematical formulation. There is a variety of optimal control algorithms depending on 1) the order of the expansion of the dynamics, 2) the order of the expansion of the cost function and 3) the existence of noise.

More precisely, if the dynamics under consideration are linear in the state and the controls, deterministic, and the cost function is quadratic with respect to states and controls, we can use one of the most established tools in control theory: the Linear Quadratic Regulator [9]. For such type of optimal control problems the dynamics are formulated as $f(\mathbf{x},\mathbf{u}) = A\mathbf{x} + B\mathbf{u}$, $F(\mathbf{x},\mathbf{u}) = 0$ and the immediate cost

E. Theodorou is with the Department of Computer Science, University of Southern California, Los Angeles, CA 90089, USA etheodor@usc.edu
FJ Valero-Cuevas is with the Department of Biomedical Engineering, and the Division of Biokinesiology and Physical Therapy, University of Southern California, Los Angleles, CA 90089, USA valero@usc.edu

978-1-4244-4124-2/10/$25.00 ©2010 IEEE

	LQR	LQG	iLQR	iLQG	DDP	SDDP
Linear Dynamics	x	x	-	-	-	-
Quadratic Cost	x	x		-	-	-
FOE of Dynamics	-		x	x	-	-
SOE of Cost	-		x	x	x	x
SOE of Dynamics	-		-	-	x	x
Deterministic	x		x	-	x	-
Stochastic	-	x	-	x	-	x

TABLE I

OPTIMAL CONTROL ALGORITHMS ACCORDING TO FIRST ORDER EXPANSION (FOE) OR SECOND ORDER EXPANSION (SOE) OF DYNAMICS AND COST FUNCTION AND THE EXISTENCE OF NOISE.

$l(\tau, \mathbf{x}(\tau), \mathbf{u}(\tau, \mathbf{x}(\tau))) = \mathbf{x}^T Q \mathbf{x} + \mathbf{u}^T R \mathbf{u}$. Under the presence of stochastic dynamics $F(\mathbf{x}, \mathbf{u}) \neq 0$, the resulting algorithm is called the Linear Gaussian Quadratic Regulator (LQG).

For nonlinear deterministic dynamical systems, expansion of the dynamics is performed and the optimal control algorithm is solved in iterative fashion. Under a first order expansions of the dynamics and a second order expansion of the immediate cost function $l(\tau, \mathbf{x}(\tau), \mathbf{u}(\tau, \mathbf{x}(\tau)))$ the derived algorithm is called Iterative Linear Quadratic Regulator (iLQR) [6]. A better approximation of dynamics up to the second order results in one of the most well know optimal control algorithm especially in the area of Robotics, Differential Dynamic Programming [5]. Both iLQR and DDP are iterative algorithms that start with an initial trajectory in states and controls $\bar{\mathbf{x}}$ and $\bar{\mathbf{u}}$ and result in an optimal trajectory $\mathbf{x}^*$, an optimal open loop control command $\mathbf{u}^*$, and a sequence of control gains $\mathbf{L}$ which are activated whenever deviations from the optimal trajectory $\mathbf{x}^*$ are observed. The difference between iLQR and DDP is that DDP provides a better approximation of the dynamics but with an additional computational cost necessary to find the second order derivatives.

In cases where noise is present in the dynamics either as multiplicative in the controls or state, or both, we have the stochastic version of iLQR and DDP, the Iterative Linear Quadratic Gaussian Regulator (iLQG) [11] and the Stochastic Differential Dynamic Programming (SDDP) [10]. Essentially SDDP contains as special cases all the previous algorithms iLQR, iLQG and DDP since it requires second order expansion of the cost and dynamics and it takes into account control and state dependent noise. This is computationally costly because second order derivatives have to be calculated. An important aspect of stochastic optimal control theory is that, in cases of additive noise, the optimal control $\mathbf{u}^*$ and the optimal control gains $\mathbf{L}$ are both independent of the noise and, therefore, the same with the corresponding deterministic solution. In cases where the noise is control or state dependent, the resulting solutions iLQG and SDDP differ from the solutions of the deterministic versions iLQR and DDP. In the table I we provide the classification of the optimal control algorithms based on the expansion of dynamics and cost function as well as the existence of noise.

In the section that follows we present iLQG algorithm by presenting the main steps and equations of this algorithm.

III. ITERATIVE STOCHASTIC OPTIMAL CONTROL

There are 4 important initial steps for the application of iLQG which are 1) the discretization of the continuous dynamics 2) the linearization of the discrete equations 3) quadratic approximation of the cost function and 4) the quadratic approximation of the value function.

Starting with the discretization step we have that $\bar{\mathbf{x}}_{t_{k+1}} = \bar{\mathbf{x}}_{t_k} + \Delta t f(\bar{\mathbf{x}}_{t_k}, \bar{\mathbf{u}}_{t_k})$. The resulting discrete dynamics are nonlinear and they are linearized around a nominal trajectory $\bar{\mathbf{x}}_{t_k}$ as follows;

$$\delta \mathbf{x}_{t_{k+1}} = A_k \mathbf{x}_{t_k} + B_k \delta \mathbf{u}_{t_k} + \Gamma_k \left(\delta \mathbf{u}_{t_k} \right) \xi_{t_k}$$

where Γ_k is the noise transition matrix that is control depended and it is defined as follows:

$$\Gamma_k \left(\delta \mathbf{u}_{t_k} \right) = \left[\begin{array}{ccc} \mathbf{c}_{1,k} + C_{1,k} \delta \mathbf{u}_{t_k} & \cdots & \mathbf{c}_{p,k} + C_{p,k} \delta \mathbf{u}_{t_k} \end{array} \right]$$

with $\mathbf{c}_{i,k} = \sqrt{dt} F^{(i)}$ and $C_{i,k} = \sqrt{dt} \partial F^{(i)} / \partial \delta \mathbf{u}$. The state and control transition matrices are expressed as: $A_k = I + dt \partial \mathbf{f} / \partial \mathbf{x}$ and $B_k = dt \partial \mathbf{f} / \partial \mathbf{u}$. The quadratic approximation of the cost function is given as follows:

$$\begin{aligned} Cost_k = q_k + \delta \mathbf{x}_{t_k}^T \mathbf{q} + \frac{1}{2} \delta \mathbf{x}_{t_k}^T Q_k \mathbf{x}_{t_k} \\ + \delta \mathbf{u}_{t_k}^T \mathbf{r} + \frac{1}{2} \delta \mathbf{u}_{t_k}^T R_k \mathbf{u}_{t_k} + \delta \mathbf{x}_{t_k}^T P_k \mathbf{u}_{t_k} \end{aligned} \quad (2)$$

where the terms : $q_k, \mathbf{q}_k \in \Re^{n \times 1}, Q_k \in \Re^{n \times n}, \mathbf{r}_k \in \Re^{m \times 1}, R_k \in \Re^{m \times m}, P_k \in \Re^{n \times m}$ are defined as: $q_k = dt \quad \ell$; $\mathbf{q}_k = dt \ \partial \ell / \partial$, $\mathbf{Q}_k = dt \ \partial^2 \ell / \partial \mathbf{x} \partial \delta \mathbf{x}$; $\mathbf{M}_k = dt \ \partial^2 \ell / \partial \mathbf{u} \partial \mathbf{x}$, $\mathbf{r}_k = dt \ \partial \ell / \partial \delta \mathbf{u}$; $R_k = dt \ \partial^2 \ell / \partial \mathbf{u} \partial \mathbf{u}$.

The value function $V_k(\delta \mathbf{x})$ is expanded up to the second order and thus is expressed as follows:

$$V_k(\delta \mathbf{x}) = s_k + \mathbf{s}_{k+1}^T \delta \mathbf{x} + \delta \mathbf{x}^T S_{k+1} \delta \mathbf{x} \quad (3)$$

After the 4 initial steps the main equations of iLQG algorithm can now be applied as it is illustrated in table III. Essentially, the initialization of the algorithm consists of an initial trajectory in states $\{\mathbf{x}_0, ..., \mathbf{x}_T\}$ and controls $\{\mathbf{u}_0, ..., \mathbf{u}_{T-1}\}$. By treating the initial trajectories as current, the nonlinear dynamics and the cost function are linearly and quadratically approximated. In addition, the value function V_k is evaluated at the current state trajectory, starting from the terminal state $\mathbf{x}_T$ and propagated backwards until $\mathbf{x}_0$.

Backward propagation of the value function is reduced to the backward propagation of the quantities $s_k \in \Re, \mathbf{s}_k \in \Re^{n\times 1}, S_k \in \Re^{n\times n}$ as it is shown in table III. The next step after the backward propagation of the value function is the computation of the control corrections $\{\delta\mathbf{u}_0,...,\delta\mathbf{u}_{T-1}\}$. These corrections are added to the current control trajectory $\{\mathbf{u}_0^i,...,\mathbf{u}_{T-1}^i\}$ and the new controls are generated $\{\mathbf{u}_0^{i+1},...,\mathbf{u}_{T-1}^{i+1}\}$. With these new controls the nonlinear dynamics are forward propagated and the new trajectory in states is created $\{\mathbf{x}_0^{i+1},...,\mathbf{x}_T^{i+1}\}$. The new trajectories in states and controls are treated as the current and the algorithm repeats with the computation of the approximations of the dynamics, the cost and the value function around these current trajectories.

The convergence of the iLQG algorithm is achieved when the cost of the current state trajectory reaches its local minimum. Since the algorithm is gradient based, during the iterations the cost of every current trajectory should decrease until it stabilizes around a local minimum. Such convergence depends on the tuning of the cost function as well as the parameter γ in the control update equation $\mathbf{u}^* = \mathbf{u}^* + \gamma \cdot \delta\mathbf{u}^*$. Furthermore the nonlinearities in the dynamics and cost function may affect the convergence of iterative optimal control methods. In this case, fine discretization reduces the approximation error of dynamics and achieves convergence.

In the next section we describe the bio-mechanical model of the index finger and we provide the application of iLQG for the control of the index finger. The task is tapping with the index finger.

TABLE II
PSEUDOCODE OF THE ILQG ALGORITHM

- **Given**:
  - An immediate cost function $\ell(\mathbf{x},\mathbf{u})$
  - A terminal cost term ϕ_{t_N}.
  - The stochastic dynamics $\mathbf{dx} = f(\mathbf{x},\mathbf{u})dt + F(\mathbf{x},\mathbf{u})\mathbf{d}\omega$
- **Repeat** until convergence:
  - Given a trajectory in states and controls $\bar{\mathbf{x}}, \bar{\mathbf{u}}$ find the quadratic approximations of the stochastic dynamics A_t, B_t, Γ_t and the quadratic approximation of the immediate cost function $\ell_o, \ell_{\mathbf{x}}, \ell_{\mathbf{xx}}, \ell_{\mathbf{uu}}, \ell_{\mathbf{ux}}$ around these trajectories.
  - Compute all the terms $H, Q_{\mathbf{u}}, G$ and g according to:

$$\mathbf{g} = \mathbf{r}_k + B_k^T s_{k+1} + \sigma^2 \sum_i C_{i,k}^T S_{k+1} c_{i,k}$$
$$G = P_k + B_k^T S_{k+1} A_k$$
$$H = \sigma^2 \sum_i C_{i,k}^T S_{k+1} C_{i,k} + B_k^T S_{k+1} B_k + R_k$$

  - Back-propagate the quadratic approximation of the value function based on the equations:

$$S_k = Q_k + A_k^T S_{k+1} A_k + L_k^T H L_k + L^k G + G^T L_k$$
$$\mathbf{s}_k = \mathbf{q}_k + A_k^T \mathbf{s}_{k+1} + L_k^T H l_k + G^T L_k + L_k^T \mathbf{g}$$
$$s_k = q_k + s_{k+1} + \frac{1}{2}\sigma^2 \sum_i c_{i,k}^T S_{k+1} c_{i,k} + \frac{1}{2} l_k^T H l_k + l_k^T \mathbf{g}$$

  - Compute $\delta\mathbf{u}_{t_k} = -H^{-1}\left(\mathbf{g} + G\delta\mathbf{x}_{t_k}\right)$
  - Update controls $\mathbf{u}^* = \mathbf{u}^* + \gamma \cdot \delta\mathbf{u}^*$
  - Get the new optimal trajectory x^* by propagating the nonlinear dynamics $\mathbf{dx} = f(\mathbf{x},\mathbf{u}^*)dt + F(\mathbf{x},\mathbf{u}^*)\mathbf{d}\omega$.
  - Set $\bar{\mathbf{x}} = \mathbf{x}^*$ and $\bar{\mathbf{u}} = \mathbf{u}^*$ and repeat.

IV. INDEX FINGER MODEL

The skeleton of the human index finger consist of 3 joints connected with 3 rigid links. The two distal joints (proximal interphalangeal (PIP) and the distal interphalangeal (DIP)) are approximated as hinge joints that can generate both flexion-extension. The metacarpophalangeal joint (MCP) is a saddle joint and it can generated flexion-extension as well as abduction-adduction.

Fingers have at least 6 muscles, and the index finger is controlled by 7. Starting with the flexors, the index finger has the *Flexor Digitorum Profundus* (FDP) and the *Flexor Digitorum Superficialis* (FDS). The *Radial Interosseous* (RI) acts on the MCP joint. Lastly, the extensor mechanism acts on all three joints. It is an interconnected network of tendons driven by two extensor muscles *Extensor Digitorum Communis* (EC) and the *Extensor Indicis Proprius* (EI), and the *Ulnar Interosseous* (UI) and *Lumbrical* (LU) muscles. We also include 4 passive tendon elements that complete this network. These passive tendons are the *Terminal Extensor* (TE), the *Radial Band* (RB) the *Ulnar Band* (UB) and the *Extensor Slip* (ES). We simulate 11 tendons in total, 7 active (i.e., driven by independently controlled muscles) and 4 passive. The length and velocity of muscle fibers is an important determinant of muscle force production. In modeling practice, the changes in tendon length (also called tendon excursions) are the means of calculating muscle fiber lengths and velocities [12]. Therefore, we present the means to calculate tendon lengths with the understanding that these produce the necessary muscle fiber lengths and velocities to implement our Hill-type muscle model (see below). The basic equation for modeling the tendon lengths L according to [2] is given by:

$$L = \theta d + 2y\left(1 - \frac{\theta/2}{\tan(\theta/2)}\right) \quad (4)$$

where d is the distance from the straight part of the tendon towards the long axis and θ is the corresponding angle rotation. The term y corresponds to the distance from the end of the straight part towards the joint centre (i.e., moment arm). This distance is measure along the axis of the bone. A second order polynomial approximation of the equation above is formulated as follows:

$$L = (b + h\theta)\theta \tag{5}$$

where b and h are constants. With the exception of FDS and FDP, the equation above is used for modeling the lengths of tendons for muscles that are involved in flexion-extension as well as for abduction-adduction. A subscript, a, will be used to denote the dependence of the tendon length of the abduction-adduction motion, with ϕ being the adduction angle.

For the FDS and FDP tendons we decided to use the more accurate model for tendon length (4) since these tendons depend on the majority of rotational variables. More precisely,the length of FDS depends on $\theta_1, \theta_2, \theta_3$ and ϕ while the length of FDP depends on θ_1, θ_2 and ϕ. Obviously, the use of approximated model (5) for the case of FDS and FDP would have caused higher approximation errors than for the case of tendons which depend only on 1 or 2 rotational variables. More precisely we will have

$$\begin{aligned} L^{FDP} &= \theta_1 d_1^{FDP} + 2y_1^{FDP}\left(1 - \frac{\theta_1/2}{\tan(\theta_1/2)}\right) \\ &+ \theta_2 d_1^{FDP} + 2y_2^{FDP}\left(1 - \frac{\theta_2/2}{\tan(\theta_2/2)}\right) \\ &+ \theta_3 d_3^{FDP} + 2y_3^{FDP}\left(1 - \frac{\theta_3/2}{\tan(\theta_3/2)}\right) \\ &+ \left(b_a^{FDP} + h_a^{FDP}\phi\right)\phi \end{aligned} \tag{6}$$

$$\begin{aligned} L^{FDS} &= \theta_1 d_1^{FDS} + 2y_1^{FDS}\left(1 - \frac{\theta_1/2}{\tan(\theta_1/2)}\right) \\ &+ \theta_2 d_1^{FDS} + 2y_2^{FDS}\left(1 - \frac{\theta_2/2}{\tan(\theta_2/2)}\right) \\ &+ \left(b_a^{FDS} + h_a^{FDS}\phi\right)\phi \end{aligned} \tag{7}$$

The tendon length mechanism for EC and TE is rather simple due to their dependence on the rotation of only one joint. The tendon extensor for EC is a function of the rotation at the DIP joint while the tendon length of TE is function of the rotation at the PIP joint.

$$L^{TE} = -r^{TE}\theta_3, \qquad L^{ES} = -r^{ES}\theta_2 \tag{8}$$

The tendon lengths of the RB and UB are functions of the rotation around the PIP joint with the addition of the terminal extensor.

$$L^{RB} = -\left(b^{RB} + h_{RB}\theta_2\right)\theta_2 + \beta^{RB}E^{TE} \tag{9}$$

$$L^{UB} = -\left(b^{UB} + h_{UB}\theta_2\right)\theta_2 + \beta^{UB}E^{TE} \tag{10}$$

For the RI the muscle length is a function of the MCP rotation only that includes flexion-extension and abduction-adduction. Therefore its tendon length is formulated as follows:

$$\begin{aligned} L^{RI} &= \left(b^{RI} + h_{RI}\theta_1\right)\theta_1 \\ &- \left(b_a^{RI} + h_a^{RI}\phi\right)\phi \end{aligned} \tag{11}$$

Similarly, the muscle length for the LI is a function of the MCP rotation but with the addition of the tendon length of the UB. Consequently its tendon length is formulated by the following equation:

$$\begin{aligned} L^{UI} &= \left(b^{UI} + h_{UI}\theta_1\right)\theta_1 \\ &+ \left(b_a^{UI} + h_a^{UI}\phi\right)\phi + L^{UB} \end{aligned} \tag{12}$$

The length of the LU muscle is a function of the MCP rotation with the addition of the UB and the subtraction of the FDP tendon lengths. The length of FDP tendon is subtracted from the total length of the LU since the origin of LU is on the FDP tendon. Thus we will have that:

$$\begin{aligned} L^{LU} &= \left(b^{LU} + h_{LU}\theta_1\right)\theta_1 \\ &- \left(b_a^{LU} + h_a^{LU}\phi\right)\phi \\ &+ L^{RB} - L^{FDP} \end{aligned} \tag{13}$$

Finally the muscle lengths of the main extensors of the index finger, EC and EI are function of the MCP rotation and with the addition of the displacements that are transformed to the next joints PIP and DIP through the extensor mechanism.

$$\begin{aligned} L^{EC} &= -r^{EC}\theta_1 - \left(b_a^{EC} + h_a^{EC}\phi\right)\phi \\ &+ \min(L_1, L_2, L_3) \end{aligned} \tag{14}$$

and

$$\begin{aligned} L^{EI} &= -r^{EI}\theta_1 + \left(b_a^{EI} + h_a^{EI}\phi\right)\phi \\ &+ \min(L_1, L_2, L_3) \end{aligned} \tag{15}$$

where the terms L_1, L_2 and L_3 are defined as $L_1 = L^{ES}$, $L_2 = L_{UB} + \left(1 - \beta^{UB}\right)L^{TE}$ and $L_3 = L_{RB} + \left(1 - \beta^{RB}\right)L^{TE}$

In this work we have slightly modified the extensor mechanics for the EI and the EC muscles to avoid the nonlinear operator min by assuming that: $L^{EC} = -r^{EC}\theta_1 - \left(b_a^{EC} + h_a^{EC}\theta_1\right)\theta_1 + E\left(L_1, L_2, L_3\right)$ and $L^{EI} = -r^{EI}\theta_1 - \left(b_a^{EI} + h_a^{EI}\phi\right)\phi + E\left(L_1, L_2, L_3\right)$ with the length function $E\left(L_1, L_2, L_3\right)$ defined as $E\left(L_1, L_2, L_3\right) = \sum_{j=1}^{3} w_j L_j$ with $\sum_{j=1}^{3} w_j = 1$ and $w_j > 0 \forall j = 1,2,3$. There are 39 parameters for the equations of the 11 tendons lengths of the index which are provided in table [2].

V. Index Finger Moment Arm

Since the lengths have been defined for the 11 tendons of the index finger, the moment arm matrix for the 7 muscles can been found according to the equation $\mathbf{M}(\Theta) = \nabla_{\boldsymbol{\Theta}}\mathbf{L}$ where $\Theta = (\theta_1, \theta_2, \theta_3, \phi)^T$ and $\mathbf{L} \in \Re^{7\times 1}$ defined as $\mathbf{L} = \left(L^{FDS}, L^{FDP}, L^{LU}, L^{RI}, L^{LU}, L^{EC}, L^{EI}\right)^T$. More precisely the moment arm vector for the FDP tendon is expressed as $\mathbf{M}_{\boldsymbol{\Theta}}^{FDP} = \left(M_{\theta_1}^{FDP}, M_{\theta_2}^{FDP}, M_{\theta_3}^{FDP}, M_{\phi}^{FDP}\right)$ where $\forall i = 1,2,3$ we have that

$$M_{\theta_i}^{FDP} = d_i^{FDP} + y_i^{FDP}\left(\frac{\sin(\theta_i) - \theta_i}{2\sin^2(\theta_i)}\right) \tag{16}$$

and $M_{\phi}^{FDP} = h_a\phi$. In cases where $\theta_i = 0$ then the moment arm of the FDP is given by the following equation $\lim_{\theta_i\to 0} M_{\theta_i}^{FDP} = d_i^{FDP}, \quad \forall i = 1,2,3$. The moment arm vector for the FDS tendon is expressed as $\mathbf{M}_{\boldsymbol{\Theta}}^{FDS} = \left(M_{\theta_1}^{FDS}, M_{\theta_2}^{FDS}, M_{\theta_3}^{FDS}, M_{\phi}^{FDS}\right)$ where $\forall i = 1,2$ we have that:

$$M_{\theta_i}^{FDS} = d_i^{FDS} + y_i^{FDS}\left(\frac{\sin(\theta_i) - \theta_i}{2\sin^2(\theta_i)}\right) \tag{17}$$

(18)

and $M_{\theta_3}^{FDS} = 0, \quad M_{\phi}^{FDS} = h_a\phi$. Similarly when $\theta_i = 0$ then the moment arm of the FDS is given by the following equation: $\lim_{\theta_i\to 0} M_{\theta_i}^{FDS} = d_i^{FDS} \forall i = 1,2$. For the LU tendon the moment arm vector is expressed as:

$$\mathbf{M}_{\boldsymbol{\Theta}}^{LU} = \begin{bmatrix} M_{\theta_1}^{LU} \\ M_{\theta_2}^{LU} \\ M_{\theta_3}^{LU} \\ M_{\phi}^{LU} \end{bmatrix} = \begin{bmatrix} b^{LU} + h^{LU}\theta_1 - M_{\theta_1}^{FDP} \\ M_{\theta_2}^{RB} - M_{\theta_2}^{FDP} \\ M_{\theta_3}^{RB} - M_{\theta_3}^{FDP} \\ -b_a^{LU} - h_a^{LU}\phi - M_{\phi}^{FDP} \end{bmatrix} \tag{19}$$

Similarly for the UI and RI tendons we will have

$$\mathbf{M}_{\boldsymbol{\Theta}}^{RI} = \begin{bmatrix} M_{\theta_1}^{RI} \\ M_{\theta_2}^{RI} \\ M_{\theta_3}^{RI} \\ M_{\phi}^{RI} \end{bmatrix} = \begin{bmatrix} b^{RI} + h^{RI}\theta_1 \\ 0 \\ 0 \\ b_a^{RI} + h_a^{RI}\phi \end{bmatrix} \tag{20}$$

and

$$\mathbf{M}_{\boldsymbol{\Theta}}^{UI} = \begin{bmatrix} M_{\theta_1}^{UI} \\ M_{\theta_2}^{UI} \\ M_{\theta_3}^{UI} \\ M_{\phi}^{UI} \end{bmatrix} = \begin{bmatrix} b^{UI} + h^{UI}\theta_1 \\ M_{\theta_2}^{UB} \\ M_{\theta_3}^{UB} \\ b_a^{UI} + h_a^{UI}\phi \end{bmatrix} \tag{21}$$

As we can see from above the moment arm vectors for UI and RI are function of the moment arm vectors of UB and RB tendons which are defined as follows

$$\mathbf{M}_{\boldsymbol{\Theta}}^{UB} = \begin{bmatrix} M_{\theta_1}^{UB} \\ M_{\theta_2}^{UB} \\ M_{\theta_3}^{UB} \\ M_{\phi}^{UB} \end{bmatrix} = \begin{bmatrix} 0 \\ -(b^{UB} + h^{UB}\theta_2) \\ -r^{TE} \\ 0 \end{bmatrix} \tag{22}$$

and

$$\mathbf{M}_{\boldsymbol{\Theta}}^{RB} = \begin{bmatrix} M_{\theta_1}^{RB} \\ M_{\theta_2}^{RB} \\ M_{\theta_3}^{RB} \\ M_{\phi}^{RB} \end{bmatrix} = \begin{bmatrix} 0 \\ -(b^{RB} + h^{RB}\theta_2) \\ -r^{TE} \\ 0 \end{bmatrix} \tag{23}$$

Finally, the moment arm vectors of the main extensor tendons *EC* and *EI* of the index finger are expresses as:

$$\mathbf{M}_{\boldsymbol{\Theta}}^{EC} = \begin{bmatrix} M_{\theta_1}^{EC} & M_{\theta_2}^{EC} & M_{\theta_3}^{EC} & M_{\phi}^{EC} \end{bmatrix}^T = \tag{24}$$

$$= \begin{bmatrix} -r^{EC} \\ -w_1 r^{ES} - w_2(b^{UB} + h^{UB}\theta_2) - w_3(b^{RB} + h^{RB}\theta_2) \\ -w_2 r^{TE} - w_3 r^{TE} \\ -b_a^{EC} + h_a^{EC}\phi \end{bmatrix} \tag{25}$$

and

$$\mathbf{M}_{\boldsymbol{\Theta}}^{EI} = \begin{bmatrix} M_{\theta_1}^{EI} & M_{\theta_2}^{EI} & M_{\theta_3}^{EI} & M_{\phi}^{EI} \end{bmatrix}^T =$$

$$= \begin{bmatrix} -r^{EI} \\ -w_1 r^{ES} - w_2(b^{UB} + h^{UB}\theta_2) - w_3(b^{RB} + h^{RB}\theta_2) \\ -w_2 r^{TE} - w_3 r^{TE} \\ -b_a^{EI} + h_a^{EI}\phi \end{bmatrix} \tag{26}$$

The moment arm matrix for the muscles $\mathbf{M}_{\boldsymbol{\Theta}}$ is therefore defined:

$$\begin{bmatrix} \mathbf{M}_{\boldsymbol{\Theta}}^{FDP} & \mathbf{M}_{\boldsymbol{\Theta}}^{FDP} & \mathbf{M}_{\boldsymbol{\Theta}}^{LU} & \mathbf{M}_{\boldsymbol{\Theta}}^{UI} & \mathbf{M}_{\boldsymbol{\Theta}}^{RI} & \mathbf{M}_{\boldsymbol{\Theta}}^{EI} & \mathbf{M}_{\boldsymbol{\Theta}}^{EC} \end{bmatrix} \tag{27}$$

Since the tendon length is a function $\Theta(t)$ the velocity with which the tendon length changes over time is given by $\frac{dL(\Theta)}{dt} = \frac{\partial L(\Theta)}{\partial\Theta}\frac{\partial\Theta}{\partial t}$. Thus we will have that:

$$\mathbf{V}\left(\Theta, \dot{\Theta}\right) = \mathbf{M}_{\boldsymbol{\Theta}} \times \dot{\Theta} \tag{28}$$

Joint	Tendons
DIP	Terminal Extensor (TE)
	Flexor Digitorum Profundus (FDP)
PIP	Extensor Slip (ES)
	Radial Band (RB)
	Ulnar Band (UB)
	Flexor digitorum superficialis (FDS)
	Flexor digitorum profundus (FDP)
MCP	Extensor digitorum Communis (EC)
	Extensor indicis (EI)
	Radial Interosseous (RI)
	Ulnar Interosseous (UI)
	Lumbrical (LU)
	Flexor digitorum superficialis (FDS)
	Flexor digitorum profundus (FDP)

TABLE III

CORRESPONDENCE OF THE 7 MUSCLES OF THE INDEX FINGER WITH THE 3 JOINTS MCP, PIP AND DIP.

where $\mathbf{M}_{\Theta} = \frac{\partial L(\Theta)}{\partial \Theta}$ is the moment arm matrix and $\dot{\Theta} = \frac{\partial \Theta}{\partial t}$ corresponds to the velocity of the length change.

VI. MUSCLE MODEL

In our simplified Hill-type muscle model [3] the torque is generated by the muscles FDS, FDP, LU, UI, RI, EC and EI. Therefore the torques are formulated as follows: $\tau = \mathbf{M}(\theta) \cdot \mathbf{T}\left(\alpha, L(\theta), V\left(\theta, \dot{\theta}\right)\right)$. The tension depends on the activation of the muscles but also varies with the

length $L = L(\theta)$ and velocity $V = V(\theta, \dot{\theta})$ of the muscle fibers. These are calculated on the basis of tendon lengths (as described above) that are function of joint angles and angular velocities of the index finger, respectively. Therefore the tension produced by each muscle and present in each tendon is mathematically formulated as follows: $\mathbf{T}\left(\alpha, L(\theta), V\left(\theta, \dot{\theta}\right)\right) = F_L(L(\theta)) \cdot F_V\left(V\left(\theta, \dot{\theta}\right)\right) \cdot \alpha + F_P(L(\theta))$ where the terms $F_L(L(\theta))$ and $F_V\left(V\left(\theta, \dot{\theta}\right)\right)$ are force functions that describe the force-length and force-velocity properties of muscles [4]. These force functions are defined as follows $F_L(L(\theta)) = \exp\left(-\frac{(L(\theta)-1.1)^2}{2 \cdot L_a^2}\right)$ and $F_p(L(\theta)) = 0$ if $(L < 1)$ or $F_p(L(\theta)) = (L(\theta) - 1)^2 L_{\beta}$ otherwise. In addition, $F_V\left(V\left(\theta, \dot{\theta}\right)\right) = \frac{2}{1+\exp\left(V\left(\theta, \dot{\theta}\right) \cdot L_d\right)}$ if $(V < 0)$ or $F_V\left(V\left(\theta, \dot{\theta}\right)\right) = 1 + \frac{2}{1+\exp\left(V\left(\theta, \dot{\theta}\right) \cdot L_d \cdot L_c\right) - 1} \frac{1}{L_c}$ otherwise. The length of the muscles is expressed in units of L_0 where L_0 is the length at which the maximum isometric force is generated [3], [4]. In addition velocity $V\left(\theta, \dot{\theta}\right)$ is expressed in units of L_0/sec. The muscle length and velocity are converted into normalized units of L_0 according to the operating length range of each one of the muscles. After specifying the moment arm of the index finger and discussing the muscle model used in this work, in the next section we provide our result on the application of stochastic optimal control for movement generation of the tendon-driven index finger.

VII. MODELING INDEX DYNAMICS AND CONTACT

We are modeling the index finger as a 3 link multi-body dynamical systems. The forward dynamics of the index finger are expressed as follows:

$$\begin{aligned} \ddot{\theta} &= -\mathbf{I}(\theta)^{-1} \mathbf{C}\left(\theta, \dot{\theta}\right) + \mathbf{I}(\theta)^{-1} \tau + \mathbf{I}(\theta)^{-1} J(\theta)^T \mathbf{F}_e \\ \tau &= \mathbf{M}(\theta) \cdot \mathbf{T}\left(\alpha, l(\theta), V\left(\theta, \dot{\theta}\right)\right) && (29) \\ \dot{a}_i &= -\frac{1}{c}(a_i + u), \quad i = 1, \ldots, 7 && (30) \end{aligned}$$

where θ and $\dot{\theta}$ are the joint position and joint velocities, a_i's are the activation variables and u_i's are the control neural signals. Moreover, $\mathbf{I}(\theta)$ is the inertia matrix, $\mathbf{C}\left(\theta, \dot{\theta}\right)$ is the vector of centripetal and coriolis forces and $J(\theta)$ is the jacobian matrix which maps the end effector force to joint torques. The forward dynamics are driven by the torques τ and the end effector force $\mathbf{F}_e$ activated during contact with a surface. The torques are driven by the 7 tensions applied through by the 7 muscles of the index finger. The matrix $\mathbf{M}$ is the moment arm matrix and the function $T(\theta, \mathbf{L}(\theta), \mathbf{V}(\dot{\theta})$ correspond to the applied tensions. The function $\mathbf{L}(\theta)$ and $\mathbf{V}(\dot{\theta})$ correspond to the tendon excursions and velocities specified in section V. The contact force $\mathbf{F}_e$ is given by a nonlinear spring damper formulation that is given as $\mathbf{F}_e(\theta, \dot{\theta}) = K_s(l_o - |y_e - y_d|) + K_d \dot{y}_e^4$ with y_e is the actual end effector position in the y direction while y_d is the desired position. The terms K_s and K_d are constants while l_o is the length of the virtual spring attached into the end effector. The force in the end effector depends on the joint angles and and joint velocity since $y_e = l_1 c_1 + l_2 c_1 2 + l_3 c_{123}$ and $\dot{y}_e = -l_1 s_1 \dot{\theta}_1 - l_2 s_{12}(\dot{\theta}_1 + \dot{\theta}_2) - l_3 s_{123}(\dot{\theta}_1 + \dot{\theta}_2 + \dot{\theta}_3)$.

We have applied the iLQG algorithm to control the index finger for the tapping task. The cost function for this task is specified as $J(\mathbf{x}) = (\theta - \theta^*)^T Q_T (\theta - \theta^*) + \frac{1}{2}\int_{t_0}^T \mathbf{u}^T R \mathbf{u} dt + \int_{t_c}^T (\theta - \theta^*)^T M (\theta - \theta^*) dt$. Essentially the cost function consists of the 3 terms. The first term penalizes deviations of the index finger from the target posture at the terminal time T. The second term penalizes the control cost over the entire time horizon and the third term penalizes deviations from the desired posture after the time $t_c = 0.275 sec$ which is the time that contact occurs. The tuning of the cost function is specified as $Q = M = 5000 I_{3\times3}$ and $R = 0.001$.

The results of our simulations are illustrated in figures 1 and 2. More precisely, in 1 the kinetics of the muscles are illustrated. As we can see for the tapping task, the flexors decrease their length while extensors increase their length as expected. Figure 2 illustrates the torques and the end effector force generated due to contact. Before contact the torques and the end effector force are zero while after contact they

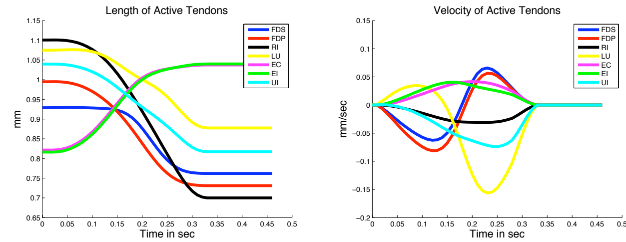

Fig. 1. The time history of the length and velocity of the muscles of the index finger for the tapping task with zero terminal velocity.

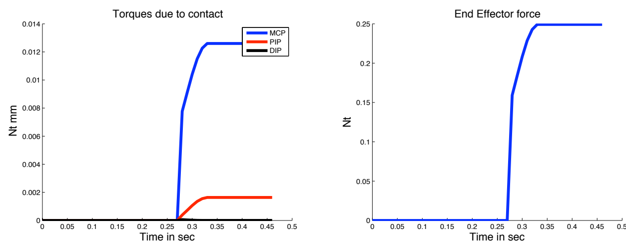

Fig. 2. The time history of the torques and the force applied to the finger due to contact.

are set to no zero values with the highest value for the torques at the MCP joint.

VIII. Conclusions

In this note, we give overview of optimal control methods based on their characteristic of the order of the expansions of dynamics and cost function. In particular we describe optimal control approaches applicable to nonlinear and stochastic dynamical systems such as realistic models of neuro-musculo-skeletal systems. We use the index finger as a sample system whose anatomical complexity has challenged prior methods. Moreover, we demonstrate the application of these optimal control methods to what, to our knowledge, is the most complex model of a tendon-driven system. Prior work has been largely limited to torque-driven systems which lack the important nonlinearity of uni-directional actuation, or to simpler tendon driven systems for which the state vector is much smaller. Therefore our work presents important extensions and innovations in the applicability of optimal control to realistic models of neuro-musculo-skeletal systems.

Many challenges remain, and the limitations of our work suggest directions for future work. For example, besides requiring accurate knowledge of the dynamics of the system and cost functions, constraints in control and state variables are very often required in neuromuscular systems. We have used heuristic methods to minimize the violation of such constraints, but the field of optimal control in general still requires a rigorous formulation and numerical approaches to robustly impose such constraints on states and controls. These constrains not only increase the computational cost of the optimal control methods, but can lead to infeasible optimization problems. In addition, validation of predictions using experimental tendon-driven systems is necessary. Before this can be done, however, optimal control methods will have to be refined to tolerate discrepancies between the model used to find control policies and the actual nonlinear dynamics of physical systems. In fact, the ability of the central nervous system to control well (even optimally?) such nonlinear, stochastic neuro-musculo-skeletal plants suggests that fundamental developments in control theory will be necessary to understand motor function in detail.

IX. Acknowledgments

This material is based upon work supported by the Myronis Scholarship to E. Theodorou, and NSF Grant 0836042, NIDRR Grant 84-133E2008-8, and NIH Grant AR050520 and Grant AR052345 to F. J. Valero-Cuevas. Its contents are solely the responsibility of the authors and do not necessarily represent the official views of the National Institute of Arthritis and Musculoskeletal and Skin Diseases (NIAMS), NIH, NSF, or NIDRR.

References

[1] T. Basar and P. Berhard. *H-infinity Optimal Control and Related Minimax Design*. Birkhauser, Boston, 1995.

[2] N Brook, Mizrahi J, Shoham M, and Dayan J. A biomechanical model of the index finger dynamics. *Medical Engineering Physics.*, 17:54–63, 1995.

[3] A Freivalds. *Biomechanics of the upper limbs: mechanics, modeling, and Musculoskeletal injures*. CRC Press, 1st edition, 2000.

[4] Brown I and Loeb G. Measured and modeled properties of the mammalian skeletal muscle IV. Dynamics of activation and deactivation . *Journal of Muscle Research and Cell Mobility*, 21:33 – 47, 2000.

[5] D. H. Jacobson and D. Q. Mayne. *Differential Dynamic Programming*. Optimal Control. Elsevier Publishing Company, New York, 1970.

[6] Weiwei Li and Emanuel Todorov. Iterative linear quadratic regulator design for nonlinear biological movement systems. In *ICINCO (1)*, pages 222–229, 2004.

[7] Frank A. Netter, John A. Craig, and James Perkins. Icon Custom Communications.

[8] S. Skogestad and I. Postlethwaite. *Multivariable Feedback Control*. Wiley, 2005.

[9] Robert F. Stengel. *Optimal control and estimation*. Dover Publications, New York, 1994.

[10] E. Theodorou, Y. Tassa, and E. Todorov. Stochastic differential dynamic programming. In *Proceedings of the American Control Conference*, 2010.

[11] E. Todorov and W. Li. A generalized iterative LQG method for locally-optimal feedback control of constrained nonlinear stochastic systems. In *Proceedings of the American Control Conference*, 2005.

[12] Francisco J. Valero-Cuevas, Heiko Hoffmann, Manish U. Kurse, Jason J. Kutch, and Evangelos A. Theodorou. Computational Models for Neuromuscular Function. *IEEE Reviews in Biomedical Engineering*, (2):110–135, October 2009.